where β is the fraction of spontaneous emission coupling into the laser mode and $R_n(n_{a,b})$ are the spontaneous carrier recombination rates in each section. In a QW laser, they can be given by $Bn_{a,b}^2$, where B is a bimolecular recombination coefficient and $n_{a,b}$ are the carrier densities.

Using the definition in eqn. 7, the R^u_{sp}/R_{sp} ratio (A_r) is written as

$$A_r = \frac{R^u_{sp}}{R_{sp}} = \frac{n_u^2}{(1-h)n_a^2 + hn_b^2} \qquad (8)$$

If $h \to 1$ then $n_b \to n_u$ and $A_r \to 1$. When $h < 1$, n_b has to increase so that eqn. 1 can be satisfied. As a consequence, the rate of spontaneous emission R_{sp} of the gain-lever laser increases and A_r decreases, resulting in the SNR improvement decreasing with h as shown in Fig. 3. It must be emphasised that this dependence on h has no connection with the gain-lever effect which is described by the factor A_i.

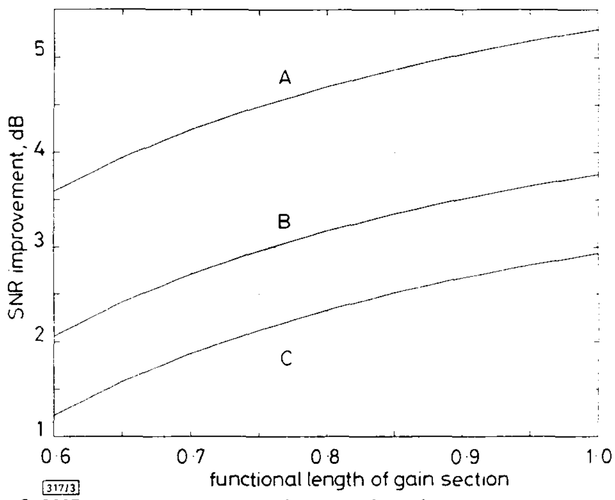

Fig. 3 *SNR improvement against h in gain-lever laser*

(i) Photon density = 1.5×10^{14} cm^{-3}
(ii) Photon density = 2.9×10^{14} cm^{-3}
(iii) Photon density = 4.2×10^{14} cm^{-3}

The SNR improvement is plotted in Fig. 3 for three values of photon density (proportional to the optical power), using a theoretical material gain curve for an AlGaAs QW [7]. The signal section is biased at 20% of the threshold gain of the laser. The maximum improvement in SNR (occurring at $h = 1$) is given by A_i. $A_i \to 1$ with increasing photon density, because the stimulated parts of the carrier inverse lifetimes γ_a and γ_u become dominant and cancel out in eqn. 6. Moreover, biasing the signal section at a low gain level increases the gain derivative and therefore improves the SNR.

Conclusion: A theoretical expression for the relative SNR improvement in a gain-lever laser is presented. This expression provides insight as to how the SNR improvement is obtained in a gain-lever laser. Either reducing the bias level to the signal section or increasing the relative length of the slave section maximises the SNR improvement. However, increasing the optical power has the opposite effect. Furthermore, the dependence of the SNR_i on the parameter h stems from the dependence of the rate of spontaneous emission R_{sp} on this parameter.

15 May 1995
Electronics Letters Online No: 19950776

J.C.S. Castro, A. Khanifar and C.J. Todd (*Department of Electronic and Electrical Engineering, University College London, Torrington Place, London WC1E 7JE, United Kingdom*)

References

1 MOORE, N., and LAU, K.Y.: 'Ultrahigh efficiency microwave signal transmission using tandem-contact single quantum well GaAlAs lasers', *Appl. Phys. Lett.*, 1989, **55**, (10), pp. 936–938

2 GAJIC, D., and LAU, K.Y.: 'Intensity noise in the ultrahigh efficiency tandem-contact quantum well lasers', *Appl. Phys. Lett.*, 1990, **57**, (18), pp. 1837–1839

3 LAU, K.Y.: 'Passive microwave fiber-optic links with gain and very low noise figure', *IEEE Photonics Technol. Lett.*, 1991, **3**, (6), pp. 557–559

4 SELTZER, C.P., WESTBROOK, L.D., and WICKES, H.J.: 'Improved signal-to-noise ratio in gain-levered InGaAs/InP lasers', *Electron. Lett.*, 1993, **29**, (2), pp. 230–231

5 AGRAWAL, G.P., and DUTTA, N.K.: 'Long-wavelength semiconductor lasers' (Van Nostrand, New York, 1986)

6 KUZNETSOV, M., WILLNER, A.E., and KAMINOW, I.P.: 'Frequency modulation response of tunable two-segment distributed feedback lasers', *Appl. Phys. Lett.*, 1989, **55**, (18), pp. 1826–1828

7 CORZINE, S.W., YAN, R.H., and COLDREN, L.A.: 'Theoretical gain in strained InGaAs/AlGaAs quantum well including valence-band mixing effects', *Appl. Phys. Lett.*, 1990, **57**, (26), pp. 2835–2837

Internal optical loss measurements in 1.3μm InGaAsP lasers

G.E. Shtengel and D.A. Ackerman

Indexing terms: Semiconductor lasers, Laser variable measurement

A highly accurate method of measuring optical loss in individual semiconductor lasers is presented and compared with other methods. Measured loss data for 1.3μm semiconductor lasers are presented that illustrate the suitability of this technique for studying the dependence of loss on temperature and carrier density.

Internal optical loss is a fundamental property of a semiconductor laser. The value of internal loss at the lasing threshold affects threshold current and external slope efficiency. The temperature dependent internal optical loss has been cited as an important factor affecting the temperature performance of long-wavelength lasers [1]. However, measurement of optical loss as a function of current, carrier density or temperature with sufficient accuracy to address issues such as these is difficult.

An early and widely used technique for measuring internal optical loss [2] requires a set of lasers, varying in length but otherwise equivalent, to estimate the average value of loss at threshold. This protocol takes into account neither the systematic variation of the threshold condition owing to variation in length (e.g. dependence of threshold density on length) nor random variation between lasers. In addition, this method precludes measurement on individual devices and measurement below threshold.

Several new techniques have recently been proposed for optical loss measurements [3–5]. They are all based on the simple relationship connecting modal gain, material gain and total loss in the laser, given by

$$G = \Gamma g - \alpha_{tot} \qquad (1)$$

in which G is the modal gain, g is the material gain, Γ is the optical confinement factor and total optical loss is the sum of the mirror and internal losses. From eqn. 1, it is clear that modal gain is equal to the total loss if the material gain is zero. This condition holds as a good approximation [4] for energies well below the bandgap energy and holds rigorously at the transparency energy, i.e. at the transition point between absorption and gain. Thus, finding the modal gain at these points provides the value of the total loss, which in turn provides internal loss if the mirror loss is known. Simple spectral contrast measurement of amplified spontaneous emission (ASE) gives the required modal gain spectra using the technique of Hakki *et al.* [6].

Techniques based on below-bandgap measurements [3, 4] are difficult because of the low intensity of ASE in this region. Typical accuracy is ~5cm^{-1}, which is good only for rough estimates of the loss value.

Other techniques reduce the problem of measuring internal loss to the task of determining the material transparency condition. One of the methods of determining transparency at a given current is to find the intersection of the gain curves in TE and TM polarisations [3], under the assumption that the optical gain in different polarisations is equal only when the material gain is zero.

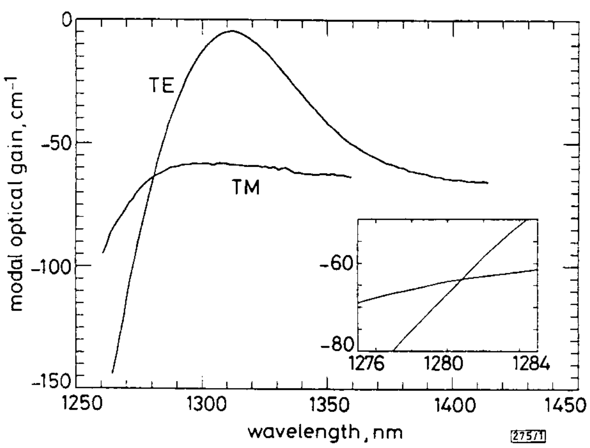

Fig. 1 *Measured TE and TM optical gains of MQW laser, I = 7mA*

Inset: close-up vicinity of intersection point

Fig. 1 shows the curves of TE-polarised gain and TM-polarised gain measured for a typical MQW laser. There is one intersection point at high energy (short wavelength) as well as indication that the two curves will converge at below-bandgap energies as the material gain tends toward zero.

Andrekson *et al.* [5] demonstrated the use of a modulated, external probe laser to find the transparency condition. In this method, an AC voltage induced on the terminals of the laser under test changes polarity when the DC bias current reaches a value corresponding to the transparency condition. (Equivalently, the wavelength of the probe laser can be tuned through transparency at a fixed DC bias current.) In our experiments using this method, in which the probe was an HP-8167A tunable external cavity semiconductor laser (ECL), we found that to achieve the required accuracy in the loss measurements, a singlemoded probe with a 10^6 side-mode suppression ratio (SMSR) was required (10^3 integrated intensity ratio). Otherwise, a parasitic effect owing to ASE from the probe, modulated at the same frequency as the probe, produces a small parasitic AC voltage across the laser terminals. Although small compared to the singlemode-induced signal, the parasitic voltage can offset the measured transparency current or wavelength. Owing to the steepness of the gain curve in this region (see inset in Fig. 1), even a very small offset of the apparent transparency current or wavelength produces considerable error in the inferred loss.

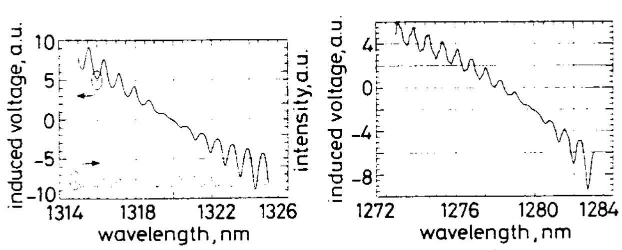

Fig. 2 *AC terminal voltage against wavelength of probe light*

a High degree of spectral purity of probe source, $I = 3$mA
b In presence of parasitic ASE from probe source, $I = 7$mA
– – – laser radiation spectra at $I = 3$mA

To avoid this parasitic effect, we measured the induced AC voltage across the laser under test while tuning the probe laser wavelength in the vicinity of the expected transparency point. Fig. 2*a* shows a typical plot of the induced voltage against ECL wavelength. Also shown in Fig. 2 (dotted line) is the ASE spectrum of the laser in this region. Corresponding features appear in both spectra owing to the Fabry-Perot cavity resonances of the laser under test, which enhance the detection properties of the laser at these wavelengths. The amplitude of the resonances in the voltage spectrum depends on the value of the material gain and equals zero at material transparency. In the absence of any parasitic probe radiation, as in Fig. 2*a*, the resonances in the voltage signal vanish at the same probe wavelength at which the induced AC voltage changes polarity. The ill-effect of parasitic radiation is illustrated in Fig. 2*b*. In this case, the ECL, operating at the edge of its range, provided insufficient suppression of its ASE of 35 dB SMSR corresponding to ~1% integrated intensity ratio. Fig. 2*b* shows an offset of ~2nm between the probe wavelengths for which the induced AC voltage equals zero and the voltage resonances vanish. This difference translates to a ~7cm^{-1} difference on a gain/loss scale. The use of a 'zero contrast' instead of a 'zero signal' criterion to find the transparency conditions avoids the error caused by inadequate spectral purity of the probe source.

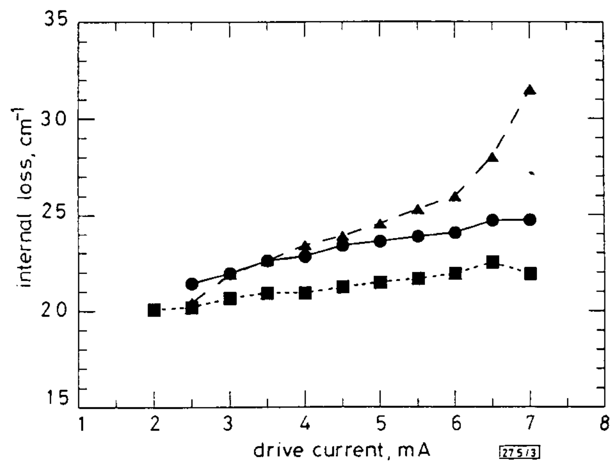

Fig. 3 *Total loss measured using three different techniques (MQW, T = 25°C)*

▲ 'zero-voltage' criterion
● 'zero-contrast' criterion
■ TE-TM crossing method

Shown in Fig. 3 are loss data measured in three ways: using the 'zero-voltage' technique of [5], using a 'zero-contrast' rather than 'zero-voltage' criterion with the same probe source, and using the TE-TM crossing method discussed above. The effect of inadequate and varying spectral purity of the probe source gives a serious error in magnitude of the internal loss and dependence on bias current as seen at the lowest and highest currents for the 'zero-voltage' set of data. The TE-TM crossing technique gives somewhat better results, underestimating the loss, but allowing data to be obtained over a slightly wider range. Errors in the loss obtained with the TE-TM crossing technique appear to be ~1nm in transparency wavelength and ~3 cm^{-1} in total loss relative to 'zero-contrast' data. We observe smoothly varying, reproducible loss data using the 'zero-contrast' method, intermediate in value to the other techniques.

In conclusion, a modification of an external probe technique for determining total loss at transparency shows accuracy of ~0.5 – 1cm^{-1}. Using a 'zero-contrast' criterion, problems associated with probe source spectral purity are avoided. This technique is also free from the confinement factor-based errors of the TE-TM crossing technique. We find that very accurate measurements such as are required for the study of the loss dependence on temperature and carrier concentration, can be obtained (and will be reported in [7]).

10 May 1995
Electronics Letters Online No: 19950764

G.E. Shtengel and D.A. Ackerman (*AT&T Bell Laboratories, Murray Hill, New Jersey 07974, USA*)

References

1 ASADA, M., and SUEMATSU, Y.: 'The effect of loss and nonradiative recombination on the temperature dependence of threshold current in 1.5–1.6mm GaInAsP/InP lasers', *IEEE J. Quantum Electron.*, 1983, **QE-19**, (6), pp. 917–923

2 CASEY, H.C., JR., PANISH, M.B., SCHLOSSER, W.O., and PAOLI, T.L.: 'GaAs-$Al_xGa_{1-x}As$ heterostructure laser with seperate optical and carrier confinement', *J. Appl. Phys.*, 1974, **45**, (1), pp. 322–333

3 AVRUTIN, E.A., CHEBUNINA, I.E., ELIASHEVITCH, I.A., GUREVICH, S.A., and SCHTENGEL, G.E.: 'TE and TM optical gains in AlGaAs/GaAs single-quantum-well lasers', *Semicond. Sci. Technol.*, 1993, **8**, (1), pp. 80–87

4 KETELSEN, L.J.P.: 'Simple technique for measuring cavity loss in semiconductor lasers', *Electron. Lett.*, 1994, **30**, (17), pp. 1422–1424

5 ANDREKSON, K.A., OLSSON, N.A., TABUN-EK, T., LOGAN, R.A., COBLENTZ, D.L., and TEMKIN, H.: 'Novel technique for determining internal loss of individual semiconductor lasers', *Electron. Lett.*, 1992, **28**, (2), pp. 171–172
6 HAKKI, B.W., and PAOLI, T.L.: 'Gain spectra in GaAs double heterostructure lasers', *J. Appl. Phys.*, 1975, **46**, (3), pp. 1299–1306
7 ACKERMAN, D.A., SCHTENGEL, G.E., HYBERTSEN, M.H., MORTON, P.A., KAZARINOV, R.F., TABUN-EK, T., and LOGAN, R.A.: 'Analysis of gain in determining T_0 in 1.3μm semiconductor lasers', *IEEE J. Quantum Electron.*, 1995, to be published in special topics issue

Noise figure and conversion efficiency of four-wave mixing in semiconductor optical amplifiers

M.A. Summerfield and R.S. Tucker

Indexing terms: Multiwave mixing, Semiconductor optical amplifiers

The noise figure of an optical frequency converter based on four-wave mixing in a semiconductor optical amplifier is defined and measured. The noise figure of the frequency converter is shown to be a function of the optical pump power, and is reduced at pump levels which are higher than the pump power required for maximum conversion efficiency.

Introduction: The efficiency of four-wave mixing (FWM) in semiconductor optical amplifiers (SOAs) is a strong function of both the amplifier gain and injected pump power [1, 2]. Owing to the compression of the gain induced by high pump power, increasing the injected pump intensity can result in a decrease in conversion efficiency [3]. Whereas the conversion efficiency has been studied in some detail, the noise performance of SOA frequency converters has received little theoretical or experimental examination. We describe and measure the effect of high pump power on noise performance.

Theory: We define the conversion efficiency η of a frequency converter by

$$\eta = \frac{I_C}{I_S} \tag{1}$$

where I_S is the input signal power and I_C is the frequency-converted output signal power. We assume that I_S is much less than the pump power I_P, and does not contribute significantly to gain compression. It has been shown that, to a first-order approximation, the conversion efficiency of FWM in an SOA is dependent on the cube of the amplifier gain and the square of the pump power [1]. That is

$$\eta \propto G^3 I_P^2 \tag{2}$$

where G is the amplifier gain. As the pump power is increased, the amplifer becomes saturated, resulting in compression of the gain. In general, the degree of gain compression is a transcendental function of the pump intensity [4]. To simplify the analysis, we propose the following empirical relationship between G and I_P:

$$G \propto I_P^{-\gamma_s} \tag{3}$$

We show that, for values of I_P of practical interest, γ_s is approximately constant. Substituting eqn. 3 in eqn. 2, the conversion efficiency can be written as

$$\eta \propto I_P^{2-3\gamma_s} \tag{4}$$

The conversion efficiency will therefore increase with increasing pump power if $\gamma_s < 2/3$, and will decrease with increasing pump power if $\gamma_s > 2/3$.

Neglecting material losses and facet reflectivities, and assuming that $G >> 1$, the power spectral density of the amplified spontaneous emission (ASE) noise is approximately proportional to the amplifier gain [5]. The frequency-converted output signal to ASE-noise ratio (SANR) depends on the input pump power according to

$$SANR \propto I_P^{2(1-\gamma_s)} \tag{5}$$

Therefore, if $\gamma_s < 1$, an increase in the pump power will result in a decrease in the output SANR.

A useful measure of the combined effect of the decreasing conversion efficiency and increasing SANR on the noise performance of the frequency converter is the noise figure (NF). We define the NF of the frequency converter as the ratio of the signal to noise ratio (SNR) of an input optical signal of photon energy $\hbar\omega$ containing only shot noise, to the SNR of the corresponding frequency-converted output signal containing shot noise and ASE noise of power spectral density W [W/Hz]. Assuming that the change in photon energy between the input and output signals is negligible, this ratio is given by

$$NF = \frac{2W + \hbar\omega}{\hbar\omega\eta} \tag{6}$$

In many applications, e.g. communications systems, it may be more important to obtain minimum NF than maximum conversion efficiency. Since the SANR increases with increasing pump power, the minimum value of NF will not, in general, coincide with the maximum conversion efficiency as a function of I_P.

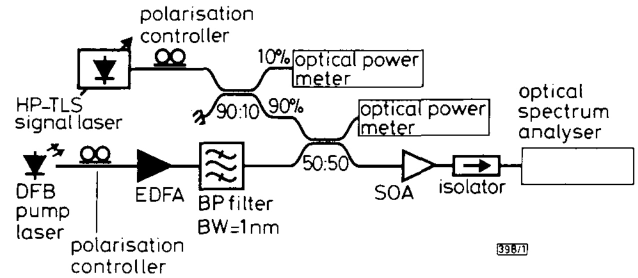

Fig. 1 *Experimental setup*

Experiment: To determine the validity of the preceding analysis, we performed an experiment to measure the NF of an SOA frequency converter. The experimental setup is shown in Fig. 1. An EDFA-amplified DFB laser with a wavelength of 1550.79nm was used as the pump source and a tunable laser source (Hewlett-Packard model 8168A) generated the input signal. The SOA is a BT&D 1100-1550. Fibre directional couplers are used to monitor the input signal, and the combined signal and pump powers. An optical spectrum analyser is used to measure the output powers and the ASE noise level into a 0.1nm resolution bandwidth.

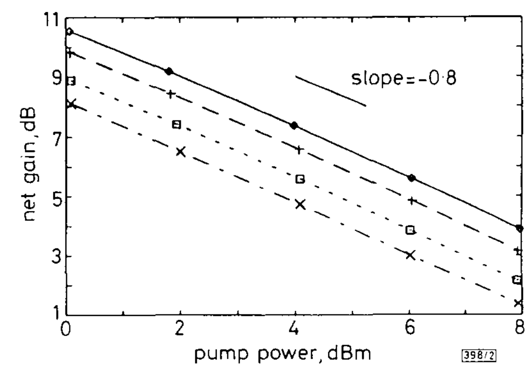

Fig. 2 *Amplifier saturation characteristics: net gain against pump power*

—◆— 180 mA SOA bias
—+— 150 mA SOA bias
- -□- - 120 mA SOA bias
- -×- - 100 mA SOA bias

The input signal power was −11.7dBm, at a wavelength of 1550.03nm, corresponding to a pump-signal detuning of ~−100GHz. Measurements were made with pump powers of 0, 2, 4, 6 and 8dBm and SOA bias currents of 100, 120, 150 and 180mA. Fig. 2 shows the measured gain of the SOA at the pump wavelength against the pump power. The curves highlight the gain compression behaviour of the SOA. Note that they are approximately linear, and in each case the data can be fitted by eqn. 3 with γ_s = 0.8, as indicated by the line of slope −0.8 in the Figure. Fig. 3*a* shows the net conversion efficiency against the input pump power for each value of SOA bias current. Towards higher pump